2326 *Biochemistry* **2010,** *49,* 2326–2334
DOI: 10.1021/bi901735a

BIOCHEMISTRY
including biophysical chemistry & molecular biology
Article

Hinge Residue I174 Is Critical for Proper dNTP Selection by DNA Polymerase β[†]

Jen Yamtich,[‡] Daniela Starcevic,[‡] Julia Lauper,[‡] Elenoe Smith,[‡] Idina Shi,[‡] Sneha Rangarajan,[§] Joachim Jaeger,[§] and Joann B. Sweasy*[,‡]

[‡]*Department of Therapeutic Radiology and Department of Genetics, Yale University School of Medicine, New Haven, Connecticut 06520, and* [§]*Wadsworth Center, New York State Department of Health, Center for Medical Science, 150 New Scotland Avenue, Albany, New York 12208*

Received October 7, 2009; Revised Manuscript Received January 4, 2010

ABSTRACT: DNA polymerase β (pol β) is the key gap-filling polymerase in base excision repair, the DNA repair pathway responsible for repairing up to 20000 endogenous lesions per cell per day. Pol β is also widely used as a model polymerase for structure and function studies, and several structural regions have been identified as being critical for the fidelity of the enzyme. One of these regions is the hydrophobic hinge, a network of hydrophobic residues located between the palm and fingers subdomains. Previous work by our lab has shown that hinge residues Y265, I260, and F272 are critical for polymerase fidelity by functioning in discrimination of the correct from incorrect dNTP during ground state binding. Our work aimed to elucidate the role of hinge residue I174 in polymerase fidelity. To study this residue, we conducted a genetic screen to identify mutants with a substitution at residue I174 that resulted in a mutator polymerase. We then chose the mutator mutant I174S for further study and found that it follows the same general kinetic pathway as and has an overall protein folding similar to that of wild-type (WT) pol β. Using single-turnover kinetic analysis, we found that I174S exhibits decreased fidelity when inserting a nucleotide opposite a template base G, and this loss of fidelity is due primarily to a loss of discrimination during ground state dNTP binding. Molecular dynamics simulations show that mutation of residue I174 to serine results in an overall tightening of the hinge region, resulting in aberrant protein dynamics and fidelity. These results point to the hinge region as being critical in the maintenance of the proper geometry of the dNTP binding pocket.

Maintenance of genomic integrity in the face of constant endogenous and exogenous DNA-damaging agents is one of the keys to healthy cell survival. As evidence of the importance of genomic stability, cancer cells are characterized by a higher mutational burden than can be accounted for by the normal cellular mutation rate (reviewed in ref *1*). This mutator phenotype can be acquired because of the loss of fidelity during DNA replication or faulty DNA repair (reviewed in ref *2*). One DNA repair pathway critical for the maintenance of genomic integrity is the base excision repair (BER) pathway, which is responsible for the repair of up to 20000 spontaneous apurinic/apyrimidinic (AP) sites per cell per day (*3*).

BER is the DNA repair pathway primarily responsible for repairing lesions caused by reactive oxygen species and alkylating agents. DNA polymerase β (pol β), an enzyme with both polymerase and deoxyribose phosphate (dRP) lyase activities, is a key enzyme in BER. It acts as the main gap-filling enzyme in both the short patch and in some cases the long patch subpathways (reviewed in ref *4*) (*5*−*8*), and the dRP lyase activity of pol β is necessary for certain subpathways as well (*9*). Pol β has been found to be mutated in approximately 30% of tumors studied to date (*10*). Several of these tumor-associated mutants have been shown to have aberrant polymerase or dRP lyase function (*11*−*13*). Additionally, some of these mutants can transform mouse cells in culture (*13*, *14*). On the basis of these and other findings, it is thought that BER may function as a tumor suppressor mechanism (reviewed in ref *15*).

In addition to its role in BER, pol β is also useful as a model for the study of polymerase activity and fidelity (reviewed in ref *4*). It follows the standard two-metal ion mechanism and is a small protein (39 kDa) that is easy to express and purify from *Escherichia coli*. Several crystal structures are available(*16*−*18*), including those of the enzyme alone and in binary and ternary complexes with a variety of substrates and nucleotides. Finally, the enzyme has no known exonuclease activity, so the observed polymerase fidelity is due strictly to the accuracy of nucleotide incorporation.

Through the use of a genetic screen capable of identifying mutator mutants of pol β (*19*), the hinge region of pol β has been shown to contain residues critical for polymerase fidelity (*19*−*22*). The hinge is a hydrophobic region of the polymerase located between the palm and finger subdomains. It has an outside lining containing residues I174, T196, and Y265 and an inner lining of residues L194, I260, and F272. These residues likely help control the enzyme's conformational change that occurs upon dNTP binding. Crystal structures show that when pol β is bound to gapped DNA it is present in an open structure and when it is bound to dNTP it is closed (*16*, *17*). Upon closing, the fingers subdomain moves approximately 12 Å (*18*). Recent studies using single-turnover kinetic analysis of mutator mutants with amino acid substitutions of hinge residues suggest that this region contributes to polymerase fidelity due to selectivity at the level of ground state dNTP binding (*21*, *23*−*25*).

While many studies have shown the importance of hinge residues in polymerase fidelity (*21*−*23*, *26*−*29*), the role of hinge

[†]This work was supported by National Institutes of Health Grant CA80830 (to J.B.S.).

*To whom correspondence should be addressed: Department of Therapeutic Radiology and Genetics, Yale University School of Medicine, New Haven, CT 06520. E-mail: joann.sweasy@yale.edu. Telephone: (203) 737-2626. Fax: (203) 785-6309.

 Published on Web 01/28/2010

residue I174 has not yet been investigated. Isoleucine 174 is located in the outside lining of the hinge and in the open conformation is in the proximity of residues Y265, T176, and K262 (Figure 1). These interactions could be interesting because Y265 has been shown to be critical for polymerase fidelity, both at the level of dNTP binding and in maintaining the substrate alignment necessary for efficient nucleotide insertion (*25*, *28*, *29*). Given its location in the hydrophobic hinge and its interaction with key hinge residues, it is important to determine what role residue I174 plays in pol β fidelity.

To further elucidate the role of the hinge in pol β fidelity, we have conducted an in-depth analysis of hinge residue I174. We began by mutating residue I174 to every other amino acid and the stop codon. We then used these variant polymerases in a genetic screen to identify mutator mutants. This screen identified the serine, threonine, aspartic acid, and glycine substitution mutants as mutators in vivo. We then chose the I174S mutant for further study and found that it is an active polymerase that has pre-steady state kinetics and folding patterns similar to those of wild-type (WT) pol β. This mutant has decreased fidelity in vitro because of a loss of discrimination at the level of ground state dNTP binding for a dTTP·G mispair and because of a combination of impaired ground state binding and chemistry for dATP·G and dGTP·G mispairs. Molecular dynamics simulations show that the observed loss of fidelity could be due to an overall tightening of the hinge region in the I174S mutant, resulting in aberrant enzyme dynamics. This tightening affects residues already known to be critical to pol β fidelity, such as Y265 and I260.

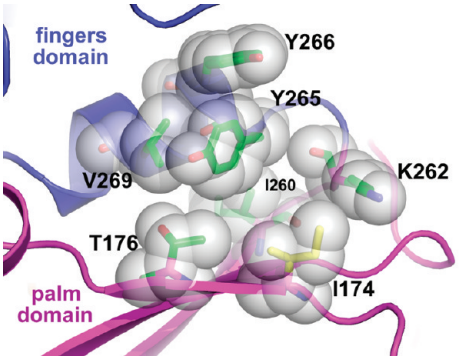

FIGURE 1: I174 and surrounding residues in the hydrophobic hinge region. Close-up view of residue I174 (yellow sticks) and neighboring side chains (green sticks) that are closely packed in this local network of interactions. The backbone cartoon is colored according to pol β subdomains (palm, magenta; fingers, blue).

MATERIALS AND METHODS

Bacterial Strains and Media. Bacterial strains and media for the tryptophan reversion assay and protein purification were used as described previously (*22*).

Chemicals and Reagents. All ultrapure deoxynucleoside triphosphates (dNTPs) were purchased from New England Biolabs. [γ-^{32}P]ATP (5 mCi) and ATP were purchased from Amersham Biosciences and Sigma-Aldrich, respectively. All oligonucleotides used for changing the I174 codon and sequencing the mutagenesis products were purchased from Keck Biotechnology Research Center at Yale University and purified by denaturing polyacrylamide gel electrophoresis (20% acrylamide and 8% urea) as described in ref *22*.

Generation of I174 Mutants. I174 mutants were generated in the rat *polB* cDNA in the pAraBAD [pBADβHis (*22*)] vector (Invitrogen) using the QuikChange site-directed mutagenesis protocol (Stratagene). For generation of mutants at position 174, primers with random nucleotides inserted at the position corresponding to the I174 codon were used [I174X-F and I174X-R, forward and reverse, respectively (Table 1)]. Polymerase chain reactions (PCRs, 50 μL) were run according to the QuikChange site-directed mutagenesis protocol using 5 ng of template DNA. PCRs consisted of an initial denaturation step at 95 °C for 30 s, followed by 16 cycles of denaturation at 95 °C for 30 s, annealing at 55 °C for 1 min, and extension at 68 °C for 10 min. To generate the I174Y, -N, -K, and -D mutants in the pBADβHis vector, the following sets of forward and reverse (F and R, respectively) primers were used: I174Y, I174N, I174K, and I174D (Table 1). To generate the I174S mutation in the pol β cDNA in the pET28a vector, the I174S forward and reverse primers were used (Table 1). To verify the generated mutations, plasmids were purified using the Qiagen Miniprep kit and sequenced with the 432+b primer that binds within the pol β cDNA sequence (Table 1) for the pBADβHis vector and with the T7 forward and terminator primers for the pET28a constructs (Table 1).

Identification of Mutator Mutants in the Trp$^+$ Reversion Screen. Mutator I174X mutants were identified using the Trp$^+$ reversion genetic screen as previously described (*22*). In short, this

Table 1: Primer Sequences[a]

Name	Sequence (5'->3')	Use
I174X-F	GCT GGA TCC CGA GTA CNN NGC TAC AGT CTG CGG CAG TTT CC	Generation of random I174
I174X-R	GGA AAC TGC CGC AGA CTG TAG CNN NGT ACT CGG GAT CCA GC	mutants in pBADβHis
I174Y-F	GCT GGA TCC CGA GTA CTA TGC TAC AGT GTG CGG CAG TTT CC	Generation of Ile174Tyr mutant in
I174Y-R	GGA AAC TGC CGC AGA CTG TAG CAT AGT ACT CGG GAT CCA GC	pBADβHis
I174N-F	GCT GGA TCC CGA GTA CAA TGC TAC AGT CTG CGG CAG TTT CC	Generation of Ile174Asn mutant in
I174N-R	GGA AAC TGC CGC AGA CTG TAG CAT TGT ACT CGG GAT CCA GC	pBADβHis
I174K-F	GCT GGA TCC CGA GTA CAA AGC TAC AGT CTG CGG CAG TTT CC	Generation of Ile174Lys mutant in
I174K-R	GGA AAC TGC CGC AGA CTG TAG CAA AGT ACT CGG GAT CCA GC	pBADβHis
I174D-F	GCT GGA TCC CGA GTA CGA CGC TAC AGT CTG CGG CAG TTT CC	Generation of Ile174Asp mutant in
I174D-R	GGA AAC TGC CGC AGA CTG TAG CGT CGT ACT CGG GAT CCA GC	pBADβHis
I174S-F	GTT AAA AAG CTG GAT CCC GAG TAC AGC GCT ACA GTC TGC GGC AGT TTC CG	Generation of Ile174Ser mutant in
I174S-R	CGG AAA CTG CCG CAG ACT GTA GCG CTG TAC TCG GGA TCC AGC TTT TTA AC	pET28a
432+b	GAA CCA CCA TCA GCG AAT TGG	Sequencing pBADβHis constructs
T7 forward	TAA TAC GAC TCA CTA TA	Sequencing pol beta pET28a+
T7 terminator	GCT AGT TAT TGC TCA GCG G	constructs

[a]Forward (F) and reverse (R) sequences (for primers used for site-directed mutagenesis and sequencing of plasmids) are listed. Underlined nucleotides represent sites of ammo acid change. For nucleotides written as N, any of the four natural nucleotides were randomly inserted by the manufacturer.

screen uses a strain of *E. coli* that is incapable of making tryptophan due to an ochre mutation in the *trpE* gene, which encodes an essential enzyme in the tryptophan synthesis pathway. Therefore, these cells need to be grown in media supplemented with tryptophan. When grown on media lacking tryptophan, a Trp^+ reversion phenotype can be observed as a result of five of six possible base substitution errors occurring by incorporation of the incorrect nucleotide into either the *trpE* gene or the anticodon loop of suppressor tRNAs. These mutations can be induced by an error-prone polymerase in the cell, such as variant forms of pol β.

DNA Substrates. DNA substrates for use in kinetic studies were prepared as described previously (*23*). Sequences of DNA substrates are listed in Table 2.

Protein Expression and Purification. Rat WT and I174S pol β proteins were expressed in *E. coli* and purified using fast protein liquid chromatography as described previously (*30*).

Pre-Steady State Burst Assay. Pre-steady state kinetic assays were conducted as described previously (*30*). In short, pol β bound to 1 bp gapped DNA substrate (100 nM enzyme and 300 nM DNA) is mixed with the correct dNTP and $MgCl_2$ in a rapid quench apparatus at 37 °C, followed by reaction quenching with EDTA on a millisecond time scale. The single base pair extended product is then separated from the unextended primer using denaturing 20% acrylamide gel electrophoresis, visualized, and quantified using a Storm 860 Phosphorimager and ImageQuant. The extended product at each time point is plotted and fit to the full burst equation

$$\frac{[P]}{[E]_0} = [E]_{app}\left\{\frac{k_2k_2}{(k_2+k_3)^2}[1-e^{-(k_2+k_3)t}]+\frac{k_2k_3}{k_2+k_3}t\right\}$$

where $[E]_{app}$ is the apparent enzyme concentration, which is proportional to the burst amplitude, k_2 is the rate of product formation, and k_3 is the rate of product release.

Circular Dichroism. Circular dichroism wavelength scans were conducted with 8 μM wild-type and I174S proteins in 10 mM K_2HPO_4 (pH 8.0). Scans were taken in crystal cuvettes with a path length of 0.1 cm thermostated at 23 °C in a Chirascan circular dichroism spectrometer (Applied Photosystems). Ellipticity was measured in 0.5 nm steps from 190 to 260 nm. Three measurements were taken for each enzyme.

In Vitro Mutagenesis Assays. Primer extension assays were conducted as described previously (*30*). In short, an excess of enzyme (750 nM WT and 1500 nM I174S) bound to 50 nM 5 bp gapped DNA was mixed with various dNTP/$MgCl_2$ mixes. Reactions were conducted for 5 min at 37 °C and quenched via addition of EDTA and 90% formamide gel loading buffer. Reaction products were separated on a sequencing gel, visualized, and quantified using a Storm 860 Phosphorimager and ImageQuant. For these assays, enzyme concentrations were based on the activity of the protein preparations derived from the presteady state burst experiments, which is proportional to the apparent enzyme concentration of the burst equation. As the active fraction of I174S was approximately half that of WT, the standard concentration of enzyme was used for WT (750 nM, 15:1 enzyme:DNA ratio) and twice the amount of enzyme was used for I174S (1500 nM). The One at a Time Primer Extension assays used only one dNTP per reaction mixture at either 12.5, 25, or 50 μM.

Single-Turnover Kinetic Assay. Single-turnover misincorporation assays were conducted as described previously (*23*). Briefly, 1 bp gapped DNA (Table 2, 45GG-U22-D22) was mixed with 750 nM enzyme so >90% of the DNA was bound. DNA binding was assessed on the basis of an apparent $K_{D(DNA)}$ of 2 nM for both WT and I174S obtained from gel electromobility shift assay results as described in ref *30* (data not shown). Reactions were initiated by mixing various concentrations of dNTP with the other reaction components and mixtures incubated at 37 °C. In cases where the incorrect dNTP was added, reaction mixtures were incubated for up to 45 min and samples were collected and quenched at multiple time points. For reactions where the correct dNTP was provided, reactions were run using a KinTek rapid quench machine for times up to 10 s. All reactions were quenched via addition of EDTA, and products were analyzed as described in Pre-Steady State Burst Assay. The concentration of extended product was then plotted against time for each reaction mixture, and the data were fit to a

Table 2: DNA Substrates[e]

DNA Substrate	Assay	Sequence
45AG-U22-D22[a]	Presteady-state burst	5' GCCTCGCAGCCGTCCAACCAAC CAACCTCGATCCAATGCCGTCC 3' CGGAGCGTCGGCAGGTTGGTTGAGTTGGAGCTAGGTTACGGCAGG
CII[b]	Missing Base Primer Extension	5' TTGCGACTTATCAACGCCCACA AGTTGTCTTCTCAGTCCT 3' AACGCTGAATAGTTGCGGGTGTAGTCATCAACAGAAGAGTCAGGA
CIIG[c]	One at a Time Primer Extension	5' TTGCGACTTATCAACGCCCACA AGTTGTCTTCTCAGTCCT 3' AACGCTGAATAGTTGCGGGTGTGGTCATCAACAGAAGAGTCAGGA
45GG-U22-D22[d]	Single Turnover Misincorporation	5' GCCTCGCAGCCGTCCAACCAAC CAACCTCGATCCAATGCCGTCC 3' CGGAGCGTCGGCAGGTTGGTTGGGTTGGAGCTAGGTTACGGCAGG

[a]The 45AG-U22-D22 substrate contains the 45-nucleotide 45AG template oligo with template A in the 1 bp gap annealed to the 22-nucleotidue U22 upstream oligo and the 22-nucleotide D22 downstream oligo. [b]The CII substrate contains the 45-nucleotide CIIT template oligo annealed to the 22-nucleotide CIIU upstream primer oligo and the 18-nucleotide CIID downstream oligo. [c]The CIIG substrate contains the same CIIU upstream primer and CIID downstream oligos used in the CII substrate annealed to the CIITG template oligo, which substitutes a template G for the first template A in the 5 bp gap found in the CII substrate. [d]The 45GG-U22-D22 substrate contains the U22 upstream primer oligo and the D22 downstream oligo used in the 45AG-U22-D22 substrate annealed to the 45GG template oligo, which substitutes a template G in the 1 bp gap compared to template A in the 45AG-U22-D22 substrate. [e]DNA substrates used for each assay are listed. Substrates are shown as annealed product with the nucleotides in the gap underlined.

single-exponential curve, yielding an observed rate constant (k_{obs}): [product] = $A(1 - e^{k_{obs}t})$. The k_{obs} values for each dNTP−enzyme combination were then plotted versus dNTP concentration, and these data were fit to a hyperbolic equation: $k_{obs} = \frac{k_{pol}[dATP]}{K_d + [dATP]}$. The rate of polymerization (k_{pol}) and the apparent dNTP binding constant (K_d) was determined for each enzyme (WT and I174S) for the insertion of each dNTP in the given 1 bp gapped sequence (Table 2, 45GG-U22-D22).

Molecular Modeling and Molecular Dynamics Simulations. Models of native and mutant pol β were generated using a high-resolution DNA cocrystal structure [Protein Data Bank (PDB) entry 2fms]. Mutations at position 174 from Ile to Ser, Thr, and Asp were introduced and modeled using VMD (*31*). The respective models were subjected to periodic-boundary molecular dynamics simulations performed for 10 ns using the Nonequilibrium Atomic Molecular Dynamics 2 (NAMD2) simulation package, version 2.6 (*32*). The Charmm27 force field was used to parametrize intramolecular interactions with long-range nonbonding terms calculated up to a 12 Å cutoff for electrostatic and van der Waals interactions. All hydrogen bond lengths were held constant with the SHAKE-RATTLE-ROLL algorithm. The TIP3P model was employed for description of the water molecules. The time step for all simulations was set to 2 fs. The simulation temperature was maintained at 310 K using a temperature bath with a coupling constant of 5 ps^{-1}. The lengths of the simulations were determined by the proper convergence of the monitored properties (typically for a period of 10 ns simulations). Trajectory analysis and molecular graphics images were generated using VMD. Root-mean-square deviation analyses were performed to evaluate system mobility and proper convergence (data not shown). Ramachandran maps, side chain dihedral analysis, and inter-residue distance scatter plots were generated to monitor and document changes in the local structure (see Figure 1) around S174/T184/D174, T176, K62, Y265, Y266, V269, Q264, and I260 over time.

RESULTS

I174S, -T, -D, and -G Are Mutator Mutants. The tryptophan reversion assay is a genetic screen used to identify mutator mutants of pol β in vivo. Our study identified four amino acid substitution mutants at I174 that result in a mutator polymerase: serine, threonine, aspartic acid, and glycine. All of these mutants showed an approximately 40-fold increase in mutation frequency compared to the wild type (Figure 2). The threonine mutant showed inconsistent results, as exemplified by the large error bars, with the majority of replicates showing a mutator phenotype. This is probably due to a decrease in the stability of the I174T mutant protein. The serine mutant was chosen for further analysis because of its consistent results across multiple replicates.

I174S and WT Share Similar Biochemical Characteristics and Protein Folding. To determine if the I174S mutant is active in vitro, we purified the His-tagged protein from *E. coli* and used the protein in a pre-steady state kinetic assay, as described in Materials and Methods. This assay is used to determine both if the protein is active and if product release is slower than nucleotide incorporation, as it is for WT pol β. Our results show that the I174S mutant is an active polymerase (for WT and I174S, k_{obs} = 11 ± 3 and 8 ± 2 s^{-1} and k_{ss} = 2 and 1 s^{-1}, respectively) that displays a biphasic burst of product formation like WT pol β (Figure 3A, inset), with a lower fraction of activity in the purified

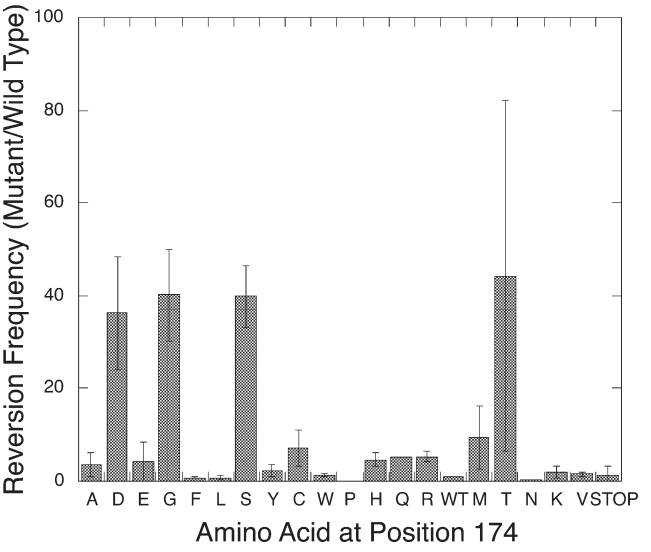

FIGURE 2: I174S, -T, -D, and -G are mutator mutants. Results of the Trp^+ reversion assay. I174 mutants are listed across the *x*-axis, and the mean mutant reversion frequency divided by the WT reversion frequency (±standard deviation) is graphed on the *y*-axis.

protein (Figure 3A, burst amplitudes of 35 and 17% for WT and I174S, respectively).

To determine if the I174S mutant has the same overall folding pattern as WT pol β, we used a circular dichroism assay. This assay showed that there are no gross structural defects in the I174S protein when compared to the wild type (Figure 3B).

I174S Is a Mutator Mutant in Vitro. To confirm the mutator phenotype of I174S identified by the in vivo Trp^+ reversion assay, we used an in vitro gap-filling primer extension assay utilizing one dNTP at a time to determine if the decreased fidelity of the I174S mutant was due primarily to misincorporation events, mispair extension, or a combination of the two. In this assay, only a single nucleotide is provided for the polymerase reactions. If the nucleotide is incorporated opposite an incorrect templating base but the mispair is not extended, then a single band should be observed at the length of the misincorporation product (for example, Figure 4A, lane 26). In this case, the polymerase is likely a misincorporation mutator. If there are multiple bands past the band for the last correct incorporation, then the mutant is likely both a misincorporator and a mispair extender (for example, Figure 4A, lane 14). If no bands are observed beyond the band representing the last correct product, then the polymerase mutant does not misincorporate. If all nucleotides are provided, pol β will conduct strand displacement synthesis and continue extending the primer beyond the 5 bp gap (Figure 4A, lanes 3−8). Results from this assay show that I174S both misincorporates and extends mispairs when inserting a pyrimidine opposite a template G (dTTP) or T (dCTP) (Figure 4A, lanes 9−20) and misincorporates but does not extend mispairs when incorporating a purine opposite template G (Figure 4A, lanes 21−32). This misincorporation and mispair extension by I174S is greater than that observed for WT pol β. For instance, for the reactions using dTTP, 85% of the total I174S reaction product is a result of misinsertion or mispair extension, whereas only 25% of the WT reaction product is due to these events (Figure 4B, quantification of lanes 13 and 14). For the case of misinsertion of a purine opposite template G, 25% of the I174S reaction product is due to misinsertion compared to only 5% of the WT reaction product (Figure 4B, quantification

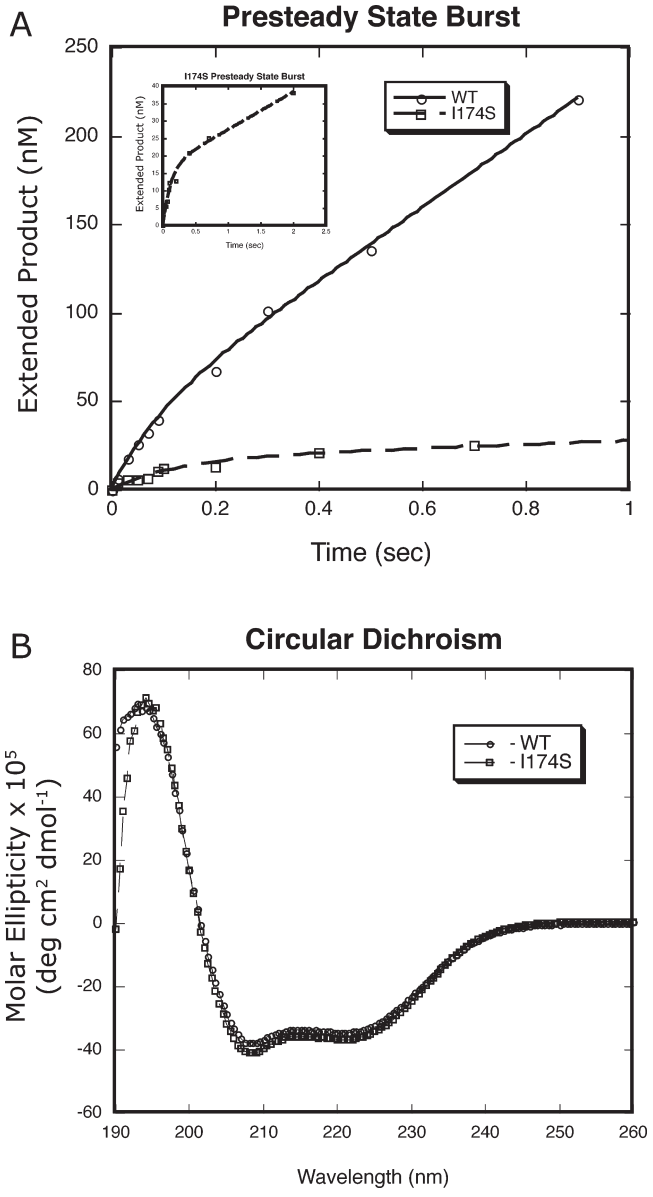

FIGURE 3: I174S and WT pol β have similar kinetic pathways and protein folding. (A) Results from a pre-steady state kinetic burst assay. The inset shows a close-up of the results for I174S, illustrating that I174S has a biphasic burst of product formation similar to that of WT. The burst rates are 11 ± 3 and 8 ± 2 s^{-1} for WT and I174S, respectively. These results are representative of multiple trials using two different protein preparations conducted at 37 °C. (B) Results from the circular dichroism assay.

of lanes 31 and 32). Given these results, we decided to investigate the mechanism underlying the I174S mutant's ability to misincorporate opposite template G using single-turnover kinetics.

I174S Lacks Discrimination at the Level of dNTP Binding. To determine which step is altered in I174S that permits it to misincorporate opposite template G more efficiently than WT, we used single-turnover kinetics. This permits us to determine the rate of polymerization (k_{pol}) and the dNTP binding affinity (K_d) for both WT and I174S when filling in a 1 bp gap with G as a templating base (Figure 5).

Using this assay, we found that I174S has a 24-fold decrease in fidelity for misinsertion of dTTP (incorrect) opposite a template G when compared to WT pol β, as shown in Table 3. Although the rates of polymerization (k_{pol}) are approximately the same for both enzymes under these conditions, I174S binds the correct nucleotide (dCTP) less tightly than the wild type while binding the incorrect dTTP more tightly, leading to a >10-fold loss in discrimination at the level of ground state dNTP binding (Table 3).

In the case of misinsertion of a purine opposite a purine (in this case, dATP and dGTP opposite template G), most of the selectivity of both WT and I174S is due to discrimination at the level of k_{pol} (Table 3). However, for the dATP opposite template G misinsertion, the discrimination at the level of k_{pol} is approximately equal for both WT and I174S and the 13-fold loss of fidelity in I174S likely results from the 8-fold loss of discrimination during dNTP binding. In the case of misinsertion of dGTP opposite G, the 11-fold loss of fidelity by I174S is likely due to loss of discrimination both at the level of k_{pol} and during dNTP binding (Table 3). Overall, these results suggest that residue I174 is important for pol β fidelity, especially at the level of ground state dNTP binding.

Molecular Dynamics Analysis Reveals a Tightening of the Hinge upon Mutation of I174. Two parallel molecular dynamics (MD) simulations were conducted with two likely serine and aspartate rotamers in the context of position 174. In the first run, the serine hydroxyl or aspartate carboxylate was facing the solvent, and in a second simulation, the side chain rotamers of the functional groups were chosen so that they faced other residues in the hinge region (away from the bulk solvent). We analyzed all trajectories in detail but chose the second scenario as the far more convincing run as far as side chain interactions and conformational changes in the surrounding local structure of the protein were concerned. For reference, the wild-type pol β structure (PDB entry 2fms) was subjected to the same protocol.

The key players involved in the local network surrounding position 174 are residues S174, T176, K62, Y265, Y266, V269, Q264, and I260 (see Figure 1). From distance analyses of these residues, it was observed that in the serine mutant, the hydroxyl group interacts with K262 and pulls the lysine toward position 174. As compared to WT, the residue 174−residue 262 distances in the S174 simulation are significantly reduced (Figure 6A). This is accompanied by a decrease in the distance between S174 and Y265, drawing them both closer. This is also supported by the fact that the distances between T176 and Y265 are considerably shorter compared to that of the WT (Figure 6A). A similar situation is found in the case of D174 (data not shown). Overall, this network of polar interactions seems to lead to a tightening of the entire hinge region.

Upon mutation of I174 to serine, there is also a marked difference in the side chain and backbone dihedrals of T176 and V178 compared to those of WT. Consequently, residues I260, Y266, and V269 show slight decreases in distance from Y265 as they move closer. Analysis of Ramachandran plots for residues 260−265, which are hinge residues adjacent to position 174 (see Figure 1), indicates that residue Q264 (and Y265 to some extent) shows a bimodal distribution of ϕ and ψ angles, a prominent difference compared to that of the WT (Figure 6B). Interestingly, however, residues 173−179 do not show any significant difference in their Ramachandran plots as compared to the WT (data not shown). Further analysis of residues lining the inside of the hinge (helix I and surrounding loops) shows that during the molecular dynamics calculations for wild-type pol β, residues Y271 and F272 both move closer to D192 and D256, while in the case of the mutants, a subtle increase in the distances is observed (Figure 6C). The concerted shifts of these bulky side chains,

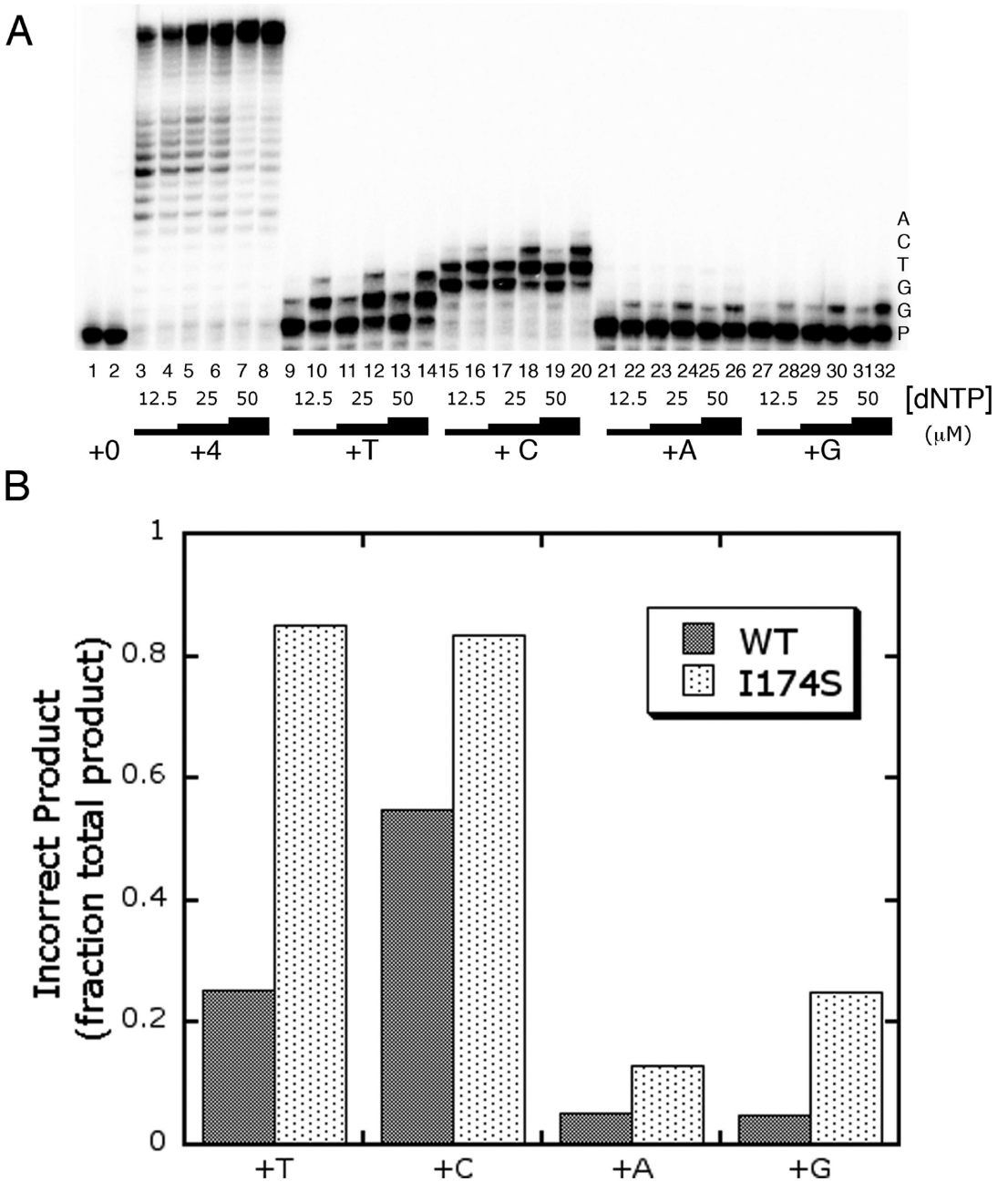

FIGURE 4: I174S has a mutator phenotype in vitro. (A) Results from the One at a Time Primer Extension assay. Reactions were conducted for 5 min at 37 °C. Odd-numbered lanes show the product from reactions using WT pol β, and even-numbered lanes show the product from I174S reactions. Nucleotides included at varying concentrations are listed along the bottom of the gel image, while the templating bases corresponding to each band of extended product are shown along the side. P stands for the band corresponding to unextended primer. (B) Quantitation of the One at at Time Primer Extension assay. Bands for reactions with the highest concentration of dNTP (50 μM) corresponding to the incorrect incorporation product from the One at a Time Primer Extension assay (A) were quantitated and presented as a fraction of total product for each reaction condition. For reactions in which dTTP, dATP, or dGTP was provided, all product longer than the primer was considered incorrect. For the reactions with dCTP incorporation, bands corresponding to insertion opposite the first two template G residues were considered correct incorporation product, and all additional bands were considered incorrect incorporation product.

which are directly adjacent to the incoming nucleotide, cause subtle changes in the shape and a small increase in the volume of the dNTP binding pocket of the mutant polymerase as compared to those of the wild-type enzyme.

DISCUSSION

Base excision repair is a DNA repair pathway critical to the maintenance of genomic integrity. DNA polymerase β acts as a key gap-filling enzyme in BER, and alterations in the polymerase fidelity could lead to an increased level of mutagenesis and eventually cancer. Previous work by our lab has suggested that certain residues of the hydrophobic hinge region of pol β are critical for accurate nucleotide insertion (*21*−*23*, *26*, *28*, *29*), thus implicating the hinge region in nucleotide discrimination. Because the hinge is a structural subdomain of pol β, we wanted to study the roles of each of its residues in nucleotide discrimination. To study the role of hinge residue I174 in pol β fidelity, we began by changing this residue to every other amino acid and screening these mutants for in vivo mutator activity. This screen identified I174S, -T, -D, and -G amino acid substitution variants as mutator mutants. We then showed that the loss of fidelity in the I174S mutant is primarily due to the loss of discrimination at the level of

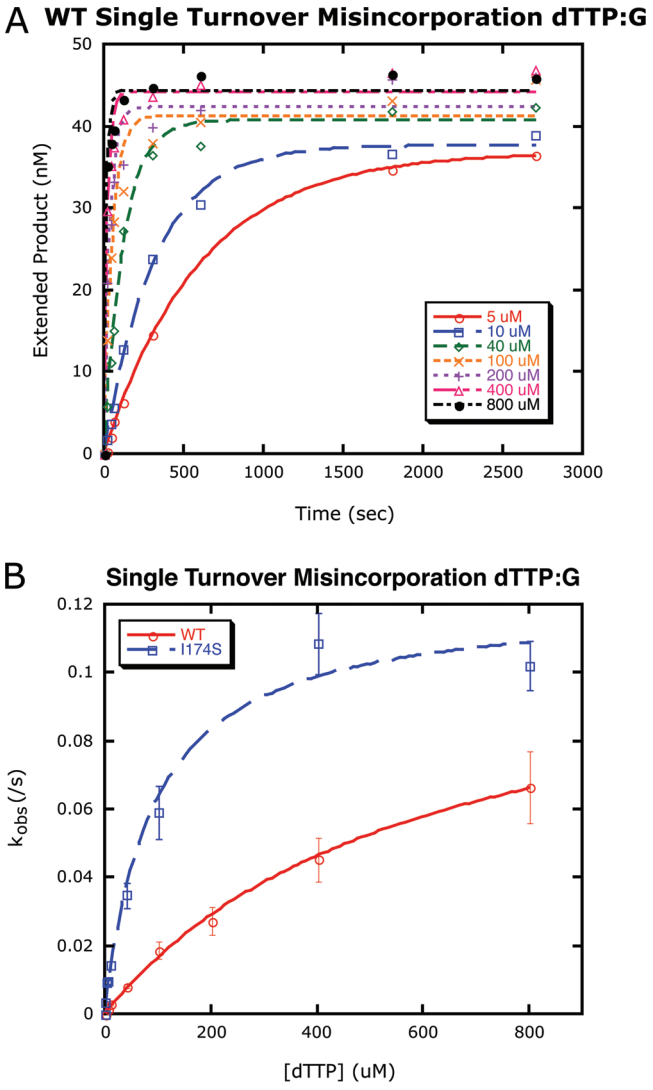

FIGURE 5: Single-turnover misincorporation opposite a template G. Representative results of a single-turnover misincorporation experiment, in this case the incorporation of dTTP opposite template G by WT. (A) For each reaction run with varying concentrations of dNTP at 37 °C, extended product was graphed against time and fit to a single-exponential curve to yield an observed rate constant. (B) The observed rate constants were plotted vs the corresponding concentration of dNTP (±standard error of the fit) and fit to a hyperbolic equation to yield the rates of polymerization and the dNTP dissociation constant for these conditions (see Table 3). Results shown are representative of the patterns of curves obtained for both WT and I174S incorporating all four dNTPs opposite a template G in a 1 bp gap.

ground state dNTP binding, especially for misinsertion of dTTP opposite a template base G. These results, in combination with our previous work, suggest that the hinge plays an important role in nucleotide discrimination at the level of ground state binding.

It is not unusual for single-amino acid substitution variants to affect pol β fidelity by altering dNTP binding. Previous studies have identified other residues that show a similar effect. These residues include Y271, which is located in the dNTP binding pocket, whose phenylalanine or serine mutants have aberrant dNTP binding (*33*). Studies involving the alanine mutant of R283, a residue that has been shown to stabilize the template DNA that is part of the dNTP binding pocket (*16*, *34*), also exhibit reduced fidelity caused by a loss of discrimination during both ground state dNTP binding and the steps reflected by the single-turnover kinetic constant, k_{pol} (*35*). Finally, two residues that bind the triphosphate moiety, R183 and R149, when mutated to alanine result in variants with decreased fidelity due to the loss of selectivity during ground state dNTP binding (*36*).

In addition to residues that occur in the dNTP binding pocket or that directly interact with the incoming dNTP, more distant residues of the hinge region have been shown to contribute to pol β fidelity by influencing dNTP binding. Mutator variants of two residues of the inner lining of the hinge were previously identified, I260Q and F272L (*21*, *22*). The F272L variant displayed a moderate mutator phenotype, misincorporating a dGTP opposite a template base A more readily than WT due to a 3-fold loss of discrimination during dNTP binding (Table 4). The I260Q variant is a strong misincorporator, with misincorporations opposite templates A and C occurring due to a 12−25-fold loss of discrimination during ground state dNTP binding compared to that of WT pol β, depending on the exact misincorporation event studied (Table 4). These results, together with our work analyzing the I174S variant, strongly suggest that the hydrophobic hinge contributes to polymerase fidelity through monitoring dNTP binding.

The loss of discrimination during ground state binding observed for the I174S mutant suggests that the mutation of a bulky hydrophobic amino acid to a smaller polar residue results in the alteration of the shape or size of the dNTP binding pocket. The fact that a small charged residue, aspartic acid, resulted in a mutator polymerase while substitution with a large polar residue, glutamic acid, did not suggests that the size of the side chain at position 174 is important for fidelity. Molecular dynamics simulations provide evidence of a mechanism by which the mutation of a hinge residue could impact the configuration of the dNTP binding pocket by showing that mutating I174 to

Table 3: Single-Turnover Kinetic Misincorporation Constants Opposite Template G[a]

dNTP	enzyme	k_{pol} (s^{-1})	K_d (μM)	k_{polc}/k_{poli}	K_{di}/K_{dc}	efficiency (μM^{-1} s^{-1})	fidelity	fold change in fidelity (WT/I174S)
dCTP	WT	8.9 ± 0.5	9 ± 2			1.0		
	I174S	6.7 ± 0.7	23 ± 6			2.9×10^{-1}		
dTTP	WT	0.115 ± 0.008	590 ± 70	78	66	1.9×10^{-4}	5155	24
	I174S	0.121 ± 0.007	90 ± 20	56	4	1.3×10^{-3}	217	
dATP	WT	0.052 ± 0.002	72 ± 9	171	8	7.3×10^{-4}	1376	13
	11745	0.093 ± 0.005	34 ± 6	73	1	2.8×10^{-3}	107	
dGTP	WT	0.0094 ± 0.0004	120 ± 10	954	13	7.9×10^{-5}	12879	11
	I174S	0.022 ± 0.001	90 ± 10	313	4	2.5×10^{-4}	1220	

[a]Kinetic constants obtained from single-turnover misincorporation assays are listed for each enzyme (±standard error). Efficiency was calculated by dividing k_{pol} by K_d for each condition. Fidelity was calculated as $[(k_{pol}/K_d)_c + (k_{pol}/K_d)_i]/[(k_{pol}/K_d)_i]$, where c and i denote the correct and incorrect dNTPs, respectively.

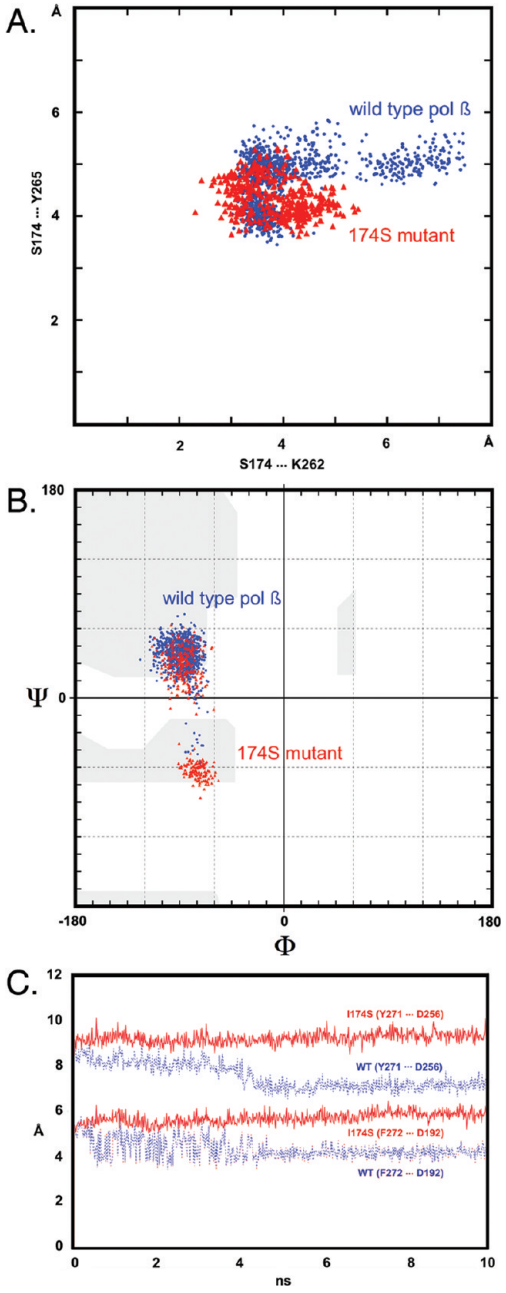

FIGURE 6: Analysis of local structural changes in the hydrophobic hinge region during a 10 ns molecular dynamics simulation. (A) Scatter plot of inter-residue distances showing Ser174 and Lys262 on the *x*-axis and Ser174 and Tyr265 along the *y*-axis. Note the overall shortening of distances and the tightening of contacts in the I174S mutant (red) simulation as compared to the pol β wild-type trajectory (blue). The network of both polar and hydrophobic interactions around the Ser174 side chain actually involves residues T176, T196, I260, K262, Y265, Y266, and V269. (B) The backbone torsion angles of residue Q264 show a bimodal distribution of ϕ and ψ angles, a prominent difference compared to that of the 174S enzyme. Changes in the peptide backbone dihedrals of hydrophobic hinge residues could affect the specific flexibility of this important region and, possibly, change the geometry of the dNTP binding pocket. (C) Distances between residues, Y271 and F272, and the catalytic aspartate residues, D192 and D256, plotted along the 10 ns MD trajectory. The distances between Y272 and D256 (top lines) and F272 and D192 (bottom) indicate that the pol β fingers domain in the wild-type calculations (dashed blue lines) has a tendency to close more tightly toward the active site than in the I174S simulation (solid red lines). The tightening of side chain−side chain interactions in the I174S mutant (see Figure 6A) appears to result in a slightly more open, perhaps less flexible fingers domain as compared to that of the wild-type structure.

Table 4: Comparison of Hinge Mutant Fidelity[a]

hinge mutant	residue location	misincorporation event	change in discrimination (WT/mutant) at k_{pol}	change in discrimination (WT/mutant) at $K_{d(dNTP)}$
I260Q(23)	inner lining	A·dATP	1.0	23
		A·dGTP	1.2	16
		A·dCTP	1.8	11
		C·dATP	1.2	18
		C·dTTP	1.3	12
		C·dCTP	1.4	25
F272L(21)	inner lining, dNTP binding pocket	A·dGTP	1.1	3.0

[a]Comparison of single-turnover kinetic constants for hinge variants that misincorporate more than WT pol β. Values for discrimination at k_{pol} and $K_{d(dNTP)}$ were taken from the referenced papers, and the ratio of discrimination for WT to mutant was calculated.

serine or aspartate in silico coincides with a marked increase in the level of mainly polar but also van der Waals interactions. These interactions cause an overall tightening of the entire network of residues consisting of S174, T176, K62, Y265, Y266, and V269.

The hydrophobic hinge is a dynamic structure that undergoes a conformational change in the course of binding dNTP (*16*). Molecular dynamics simulations reveal that along with the tightening, or altered positioning, of the surface hinge residues upon mutation of I174 to serine or aspartate, the movement, or dynamics, of interior residues relative to the palm subdomain is altered as well. Namely, the side chains of Y271 and F272, which both line the DNA binding cleft and interact with the incoming nucleotide, have decreased mobility in the 174S and 174D simulations relative to that observed in the WT simulation. This alteration of the subtle movements of the Y271 and F272 side chains caused by the tightening of the surface residues could directly alter the size and shape of the dNTP binding pocket and may, therefore, allow noncognate dNTPs to bind more readily to the mutant active site.

A similar situation was suggested to occur in the case of the I260Q and I260M mutator hinge mutants (*12*, *23*). A small cavity adjacent to I260 was shown to disappear upon mutation to glutamine or methionine. This small cavity is thought to accommodate local motions that occur upon complete closure of the fingers subdomain, and without this pocket, the hinge region may no longer be capable of completely closing the fingers subdomain around the nascent base pair. Consequently, the size and shape of the dNTP pocket would be altered, presumably leading to a change in the ground state binding of noncognate nucleotides. The combined analysis of aberrant fidelity in hinge mutants suggests a common underlying structural principle that lowered fidelity in pol β stems from small but significant restrictions in the movement of the fingers subdomain. Despite the differences in cause (mutator I174S or I260Q), the net effect is the same: weakened discrimination during ground state binding and accommodation of non-Watson−Crick base pairs in the active site of mutator mutants.

Understanding the impact of residues distant from the polymerase active site on polymerase fidelity is crucial for determining how polymerases maintain genomic stability on a regular basis. Additionally, this structural knowledge can provide insight into the role of tumor-associated mutants with substitutions found in

well-characterized regions. For instance, the I260M prostate cancer-associated hinge mutant was shown to be a sequence-specific mutator (*12*), a finding consistent with the role of the hydrophobic hinge in the maintenance of pol β fidelity. With the knowledge of how each structure in a polymerase contributes to its activity and fidelity, we can understand how a normal polymerase maintains genomic stability and how a mutated polymerase contributes to a cancer phenotype.

REFERENCES

1. Loeb, L. A. (2001) A mutator phenotype in cancer. *Cancer Res. 61*, 3230–3239.
2. Venkatesan, R. N., Bielas, J. H., and Loeb, L. A. (2006) Generation of mutator mutants during carcinogenesis. *DNA Repair 5*, 294–302.
3. Barnes, D. E., and Lindahl, T. (2004) Repair and genetic consequences of endogenous DNA base damage in mammalian cells. *Annu. Rev. Genet. 38*, 445–476.
4. Beard, W. A., and Wilson, S. H. (2006) Structure and mechanism of DNA polymerase β. *Chem. Rev. 106*, 361–382.
5. Klungland, A., and Lindahl, T. (1997) Second pathway for completion of human DNA base excision-repair: reconstitution with purified proteins and requirement for DNase IV (FEN1). *EMBO J. 16*, 3341–3348.
6. Dantzer, F., de La Rubia, G., Menissier-De Murcia, J., Hostomsky, Z., de Murcia, G., and Schreiber, V. (2000) Base excision repair is impaired in mammalian cells lacking poly(ADP-ribose) polymerase-1. *Biochemistry 39*, 7559–7569.
7. Dianov, G. L., Prasad, R., Wilson, S. H., and Bohr, V. A. (1999) Role of DNA polymerase β in the excision step of long patch mammalian base excision repair. *J. Biol. Chem. 274*, 13741–13743.
8. Prasad, R., Dianov, G. L., Bohr, V. A., and Wilson, S. H. (2000) FEN1 stimulation of DNA polymerase β mediates an excision step in mammalian long patch base excision repair. *J. Biol. Chem. 275*, 4460–4466.
9. Wiederhold, L., Leppard, J. B., Kedar, P., Karimi-Busheri, F., Rasouli-Nia, A., Weinfeld, M., Tomkinson, A. E., Izumi, T., Prasad, R., Wilson, S. H., Mitra, S., and Hazra, T. K. (2004) AP endonuclease-independent DNA base excision repair in human cells. *Mol. Cell 15*, 209–220.
10. Starcevic, D., Dalal, S., and Sweasy, J. B. (2004) Is there a link between DNA polymerase β and cancer? *Cell Cycle 3*, 998–1001.
11. Lang, T., Maitra, M., Starcevic, D., Li, S. X., and Sweasy, J. B. (2004) A DNA polymerase β mutant from colon cancer cells induces mutations. *Proc. Natl. Acad. Sci. U.S.A. 101*, 6074–6079.
12. Dalal, S., Hile, S., Eckert, K. A., Sun, K. W., Starcevic, D., and Sweasy, J. B. (2005) Prostate-cancer-associated I260M variant of DNA polymerase β is a sequence-specific mutator. *Biochemistry 44*, 15664–15673.
13. Lang, T., Dalal, S., Chikova, A., DiMaio, D., and Sweasy, J. B. (2007) The E295K DNA polymerase β gastric cancer-associated variant interferes with base excision repair and induces cellular transformation. *Mol. Cell. Biol. 27*, 5587–5596.
14. Sweasy, J. B., Lang, T., Starcevic, D., Sun, K. W., Lai, C. C., Dimaio, D., and Dalal, S. (2005) Expression of DNA polymerase β cancer-associated variants in mouse cells results in cellular transformation. *Proc. Natl. Acad. Sci. U.S.A. 102*, 14350–14355.
15. Sweasy, J. B., Lang, T., and DiMaio, D. (2006) Is base excision repair a tumor suppressor mechanism? *Cell Cycle 5*, 250–259.
16. Sawaya, M. R., Prasad, R., Wilson, S. H., Kraut, J., and Pelletier, H. (1997) Crystal structures of human DNA polymerase β complexed with gapped and nicked DNA: Evidence for an induced fit mechanism. *Biochemistry 36*, 11205–11215.
17. Pelletier, H., Sawaya, M. R., Kumar, A., Wilson, S. H., and Kraut, J. (1994) Structures of ternary complexes of rat DNA polymerase β, a DNA template-primer, and ddCTP. *Science 264*, 1891–1903.
18. Sawaya, M. R., Pelletier, H., Kumar, A., Wilson, S. H., and Kraut, J. (1994) Crystal structure of rat DNA polymerase β: Evidence for a common polymerase mechanism. *Science 264*, 1930–1935.
19. Sweasy, J. B., and Yoon, M. S. (1995) Characterization of DNA polymerase β mutants with amino acid substitutions located in the C-terminal portion of the enzyme. *Mol. Gen. Genet. 248*, 217–224.
20. Washington, S. L., Yoon, M. S., Chagovetz, A. M., Li, S. X., Clairmont, C. A., Preston, B. D., Eckert, K. A., and Sweasy, J. B. (1997) A genetic system to identify DNA polymerase β mutator mutants. *Proc. Natl. Acad. Sci. U.S.A. 94*, 1321–1326.
21. Li, S. X., Vaccaro, J. A., and Sweasy, J. B. (1999) Involvement of phenylalanine 272 of DNA polymerase β in discriminating between correct and incorrect deoxynucleoside triphosphates. *Biochemistry 38*, 4800–4808.
22. Starcevic, D., Dalal, S., and Sweasy, J. (2005) Hinge residue Ile260 of DNA polymerase β is important for enzyme activity and fidelity. *Biochemistry 44*, 3775–3784.
23. Starcevic, D., Dalal, S., Jaeger, J., and Sweasy, J. B. (2005) The hydrophobic hinge region of rat DNA polymerase β is critical for substrate binding pocket geometry. *J. Biol. Chem. 280*, 28388–28393.
24. Dalal, S., Starcevic, D., Jaeger, J., and Sweasy, J. B. (2008) The I260Q variant of DNA polymerase β extends mispaired primer termini due to its increased affinity for deoxynucleotide triphosphate substrates. *Biochemistry 47*, 12118–12125.
25. Shah, A. M., Maitra, M., and Sweasy, J. B. (2003) Variants of DNA polymerase β extend mispaired DNA due to increased affinity for nucleotide substrate. *Biochemistry 42*, 10709–10717.
26. Clairmont, C. A., Narayanan, L., Sun, K. W., Glazer, P. M., and Sweasy, J. B. (1999) The Tyr-265-to-Cys mutator mutant of DNA polymerase β induces a mutator phenotype in mouse LN12 cells. *Proc. Natl. Acad. Sci. U.S.A. 96*, 9580–9585.
27. Opresko, P. L., Shiman, R., and Eckert, K. A. (2000) Hydrophobic interactions in the hinge domain of DNA polymerase β are important but not sufficient for maintaining fidelity of DNA synthesis. *Biochemistry 39*, 11399–11407.
28. Opresko, P. L., Sweasy, J. B., and Eckert, K. A. (1998) The mutator form of polymerase β with amino acid substitution at tyrosine 265 in the hinge region displays an increase in both base substitution and frame shift errors. *Biochemistry 37*, 2111–2119.
29. Shah, A. M., Li, S. X., Anderson, K. S., and Sweasy, J. B. (2001) Y265H mutator mutant of DNA polymerase β. Proper teometric alignment is critical for fidelity. *J. Biol. Chem. 276*, 10824–10831.
30. Murphy, D. L., Kosa, J., Jaeger, J., and Sweasy, J. B. (2008) The Asp285 variant of DNA polymerase β extends mispaired primer termini via increased nucleotide binding. *Biochemistry 47*, 8048–8057.
31. Humphrey, W., Dalke, A., and Schulten, K. (1996) VMD: Visual molecular dynamics. *J. Mol. Graphics 14*, 27–38.
32. Kalé, L., Skeel, R., Bhandarkar, M., Brunner, R., Gursoy, A., Krawetz, N., Phillips, J., Shinozaki, A., Varadarajan, K., and Schulten, K. (1999) NAMD2: Greater scalability for parallel molecular dynamics. *J. Comput. Phys. 151*, 283–312.
33. Kraynov, V. S., Werneburg, B. G., Zhong, X., Lee, H., Ahn, J., and Tsai, M. D. (1997) DNA polymerase β: Analysis of the contributions of tyrosine-271 and asparagine-279 to substrate specificity and fidelity of DNA replication by pre-steady-state kinetics. *Biochem. J. 323*, 103–111.
34. Werneburg, B. G., Ahn, J., Zhong, X., Hondal, R. J., Kraynov, V. S., and Tsai, M. D. (1996) DNA polymerase β: Pre-steady-state kinetic analysis and roles of arginine-283 in catalysis and fidelity. *Biochemistry 35*, 7041–7050.
35. Ahn, J., Werneburg, B. G., and Tsai, M. D. (1997) DNA polymerase β: Structure-fidelity relationship from pre-steady-state kinetic analyses of all possible correct and incorrect base pairs for wild type and R283A mutant. *Biochemistry 36*, 1100–1107.
36. Kraynov, V. S., Showalter, A. K., Liu, J., Zhong, X., and Tsai, M. D. (2000) DNA polymerase β: Contributions of template-positioning and dNTP triphosphate-binding residues to catalysis and fidelity. *Biochemistry 39*, 16008–16015.